Journal of Statistical Physics, Vol. 54, Nos. 5/6, 1989

Deterministic and Stochastic Effects Near the Convective Onset

Guenter Ahlers,[1] Christopher W. Meyer,[1] and David S. Cannell[1]

Received April 28, 1988

The pure conduction state of a horizontal layer of fluid heated from below becomes unstable with respect to a convecting state when the temperature difference exceeds a critical value. We examine the question of how real, physical systems evolve from conduction to convection. Most experimental cells contain geometric or thermal inhomogeneities which render the bifurcation to convection imperfect. In that case the pure conduction state never exists and the convecting state evolves continuously and smoothly as the temperature difference is raised. When a sufficiently perfect experimental cell is constructed to eliminate this route to convection, then dynamic imperfections will usually prevail. When the temperature difference across the cell is raised, the vertical gradients in the sidewalls evolve at a rate which differs from that in the fluid. The resulting *transient* horizontal thermal gradients initiate the convective flow. This phenomenon can be eliminated by providing sidewalls which have the same thermal diffusivity as that of the fluid. When that is done, the convective flow is started by random noise which exists in any experimental system. Analysis of experiments shows that the noise source is considerably stronger than thermal noise, but its origin is unclear at this time.

KEY WORDS: Convection; bifurcations; stochastic effects; imperfect bifurcations; dynamic forcing; static imperfections; attractors; modulation; pattern competition.

In an ideal, laterally infinite horizontal layer of fluid heated from below, an exchange of stability between pure conduction and a convecting state occurs when the Rayleigh number R is raised above its critical value R_c (R is proportional to the temperature difference ΔT between the top and bottom of the layer).[1] The conducting state remains a solution of the

[1] Department of Physics, University of California, Santa Barbara, California 93106.

0022-4715/89/0300-1121$06.00/0

equations of motion, but it is unstable. A finite perturbation of the system is thus required if it is to evolve to the stable convecting state in a finite time. In this paper we address the question of how a real, physical system evolves from conduction to convection.

Most experimental cells contain geometric or thermal inhomogeneities which render the bifurcation at R_c imperfect. These inhomogeneities may, for instance, take the form of a nonuniform thickness of the fluid layer, a deviation from horizontality, imperfect thermal attachment of the sidewalls to the top or bottom plate, or other sources of horizontal thermal gradients near the walls.[2] In their presence the pure conduction state does not exist, and a finite though perhaps very small velocity field starts to evolve as R exceeds zero. A well-known example in the literature is the subcritical concentric convection rolls observed by Koschmieder and Pallas[3] in a fluid layer of circular cross section. Such a cylindrical pattern can be

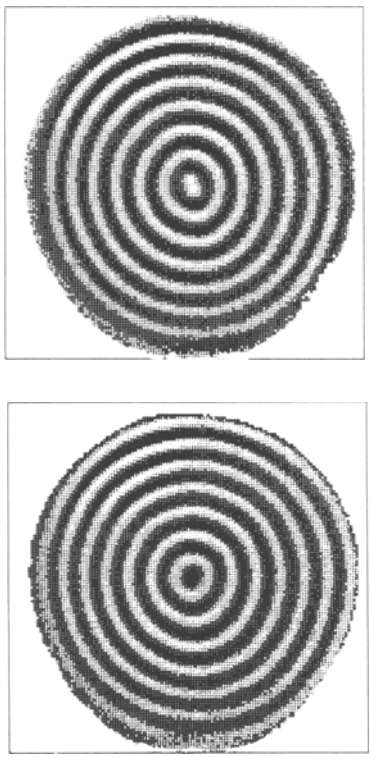

Fig. 1. Circular convection patterns stabilized by horizontal temperature gradients near the sidewalls. In both cases, $\varepsilon = 0.27$. Top: inward-pointing radial temperature gradient. Bottom: outward-pointing radial temperature gradient.

stabilized by radial temperature gradients, and the range of R over which it is stable depends upon the size of those gradients.[4] The top portion of Fig. 1 shows a shadowgraph image of such a pattern in the presence of an inward-pointing gradient.[5] In that particular case, there are seven pairs of rolls along a radius, and the flow at the center is downward (light). The pattern in the bottom portion of the figure was created by deliberately introducing an outward-pointing thermal gradient before R was raised from below to above R_c. In that case, there are also seven pairs along the radius; but the flow field is reversed and the flow at the center, for instance, is upward (dark).

The type of bifurcation leading to the patterns in Fig. 1 can be illustrated by the Landau amplitude equation

$$\tau_0(dA/dt) = \varepsilon A - A^3 + h \tag{1}$$

Here t is the time and A might be thought of as the amplitude of the radially-varying velocity field. The control parameter ε is equal to $R/R_c - 1$ or $\Delta T/\Delta T_c - 1$. The inhomogeneous term h represents the imperfections. In order to adequately describe some particular physical cases, it may of course be necessary to assume that h depends upon R, for instance in the form $h = h_0(1+\varepsilon)$. For $h=0$, the equation has the solution $A=0$, which corresponds to the conducting state. It is stable for $\varepsilon<0$ and unstable for $\varepsilon>0$. The stable solutions for $\varepsilon>0$ are $A = \pm\varepsilon^{1/2}$, and correspond to the two flow fields illustrated in Fig. 1. The solutions to Eq. (1) for $h=0$ are shown in Fig. 2a. For $h\neq 0$, the bifurcation is altered and imperfect. For sufficiently negative ε where A is small, one has $A = -h/\varepsilon$. Thus, even *well* below the bifurcation point $\varepsilon=0$ of the perfect system there is *some* flow, and the pure conduction state no longer exists. At $\varepsilon=0$, the amplitude has grown to $A = h^{1/3}$. The finite value of A at $\varepsilon=0$ corresponds to a finite convective heat transport proportional to A^2. This is reflected in a "rounding" of the Nusselt number N versus ε, as reported in some experiments.[6] For $\varepsilon>0$, A grows smoothly with increasing ε and approaches the solution $\varepsilon^{1/2}$ of the perfect system, as illustrated in Fig. 2b. The solution corresponding to the $h=0$ case $A = -\varepsilon^{1/2}$ is no longer connected to the stable solution for $\varepsilon<0$, and cannot be reached by quasistatic means. Access to it can be gained by appropriate finite perturbations, however.[7] It is connected to the unstable branch for positive ε, and has formed a saddle node at $\varepsilon = 3(h/2)^{2/3}$, $A = -(h/2)^{1/3}$. If the sign of h is changed, the lower branch will be accessible from the state at $\varepsilon<0$ and the upper branch will be inaccessible by quasistatic means. The two cases $h>0$ and $h<0$ correspond to the positive and negative radial thermal gradients used to form the two patterns in Fig. 1.

It is possible to build convection cells in which the *static* forcing effects discussed above are virtually eliminated. This is documented by heat transport measurements which in some cases have shown that the convective heat transport [which is proportional to A^2 in Eq. (1)] contributes less than 0.1% to the total heat transport at $\varepsilon = 0$.[4,8] In that case the evolving pattern may be determined by deterministic forcing effects associated with the *dynamics* of the system.[9–11] These effects often are attributable to horizontal thermal gradients near the sidewalls which arise while ε changes and because the thermal diffusivity of the walls differs from that of the fluid. In Eq. (1), they may be represented by writing the field h as $h = h_0(d\varepsilon/dt)$. In that case, the stationary solutions of Eq. (1) correspond to a perfect bifurcation and the *dynamic* field provides the perturbation which is necessary for the system to evolve from the unstable conducting to the convecting state after ε has grown to positive values. This dynamic forcing

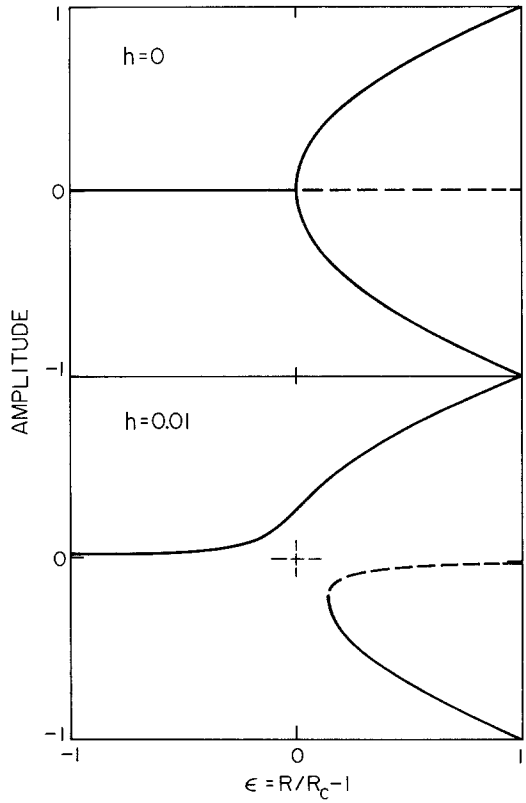

Fig. 2. Solutions to Eq. (1) with $h = 0$ (top) and $h > 0$ (bottom). Solid lines: stable solutions. Dashed lines: unstable solutions.

effect has been used to create concentric flow patterns in a study of their stability[4,5] and of wavenumber selection processes.[4] Dynamic sidewall forcing is illustrated in Fig. 3, which is for a rectangular container. In that case the heat current was changed suddenly from below to above its critical value. Initially the pattern forms primarily with rolls parallel to the sidewalls (top example, $t = 10$; the time t is in units of the vertical thermal diffusion time d^2/κ). This pattern becomes a transient in the absence of forcing, however, and evolves to a stable state after the temperature difference (ε) ceases to change. The final stable pattern, reached near $t = 120$, has a large proportion of convection rolls terminating perpendicular to the sidewalls, which is the preferred case in the absence of sidewall forcing.[4,5,12,13]

Since nearly all sidewall materials have thermal diffusivities which differ from those of the fluids, it has been quite difficult to eliminate dynamic sidewall forcing as the major factor in the pattern-formation process.

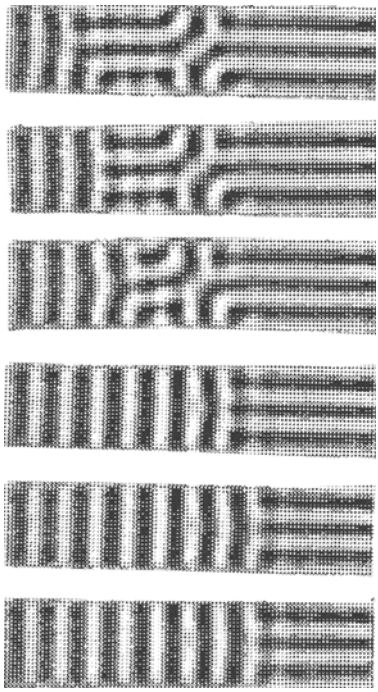

Fig. 3. Evolution of the convection pattern formed in the presence of dynamic sidewall forcing in a rectangular container. From top to bottom, the images correspond to times $t = 10$, 38, 65, 93, 120, and 1160 vertical thermal diffusion times after the temperature difference was raised suddenly from below critical to $\varepsilon = 0.56$.

Recently, however, it has been possible nonetheless to reduce the effect to a negligible level by two different wall designs.[14] One of these involved water as the working fluid, and a gel as the sidewall material. The gel was 95% water, and thus had nearly the same thermal conductivity and diffusivity as those of the working fluid. The other utilized a thin, horizontal protrusion into the cell at half height along the circumference which prevented convection near the solid walls. The effective walls were thus the nonconvecting fluid near the actual walls, and had of course the same thermal properties as the working fluid. When ε was raised gradually from below to above zero with these walls in place, patterns like that shown in the lower half of Fig. 4 evolved. They consisted of many small convective cells which apparently were randomly distributed throughout the sample. The pattern was qualitatively similar, but irreproducible in detail, in

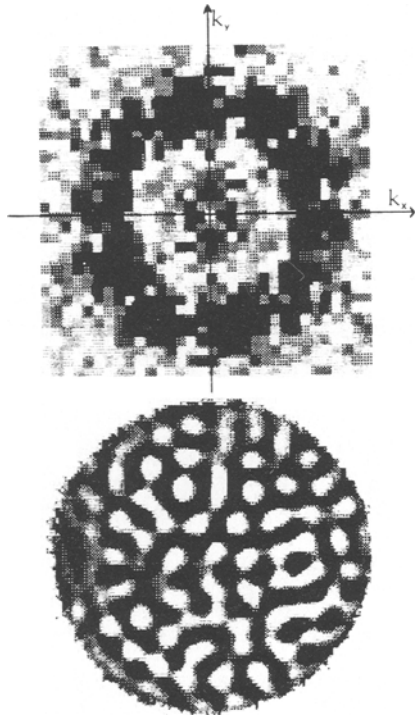

Fig. 4. Bottom: an example for a convection pattern which formed when ε was raised slowly from below to above zero in the absence of significant sidewall forcing. The pattern consists of randomly positioned cells, and is irreproducible from one experimental run to the next. Top: the different levels of grey show the absolute value of the Fourier transform of the pattern as a function of the wave-vector components k_x and k_y. The existence of a ring rather than spots reflects the random nature of the pattern.

successive runs. Thus it appears that the various deterministic dynamic and static forcing fields have been reduced to a negligible level and that stochastic effects[9,15,16] control the pattern formation. The random spatial distribution of the pattern is reflected in the top portion of Fig. 4, which is a representation of the absolute value of the Fourier transform of the pattern. A regular geometric arrangement of cellular flow would have resulted in distinct spots, whereas this pattern yielded an essentially continuous ring. There is, however, a characteristic cell size corresponding to the radius of the ring.

Another set of experimental results is shown in Fig. 5. In the bottom

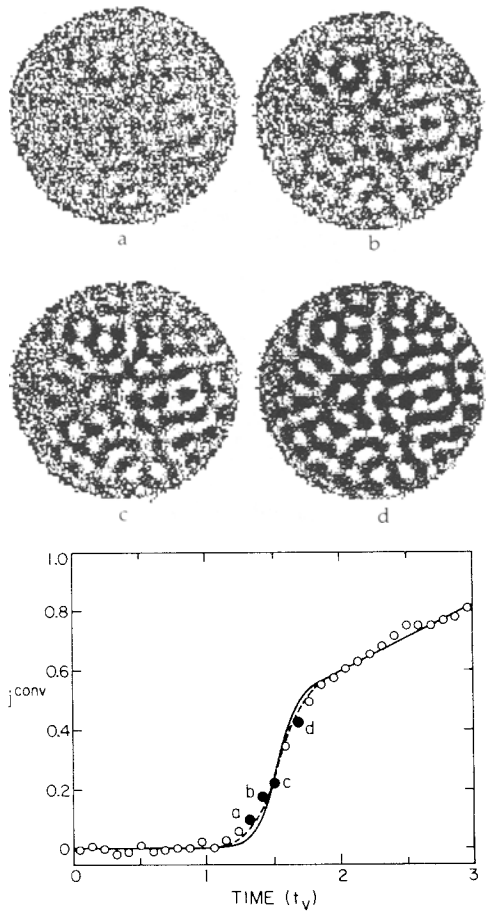

Fig. 5. (Top) emerging patterns and (bottom) data for the convective heat flux j^{conv}, as a function of time, resulting from a linear ramp $j = j_0 + \beta t$ with $\beta = 0.27$, for a cell with negligible sidewall forcing. The patterns a–d correspond to the points a–d in the bottom graph.

half of that figure the convective heat transport $j^{\text{conv}} = A^2$ is given as a function of time. Here the total heat current j was ramped linearly in time, i.e., $j = j_0 + \beta t$. The time origin was chosen so that the bifurcation point $\varepsilon = 0$ was passed at $t = 0$; but noticeable convection did not occure until $t \approx 1.3$. The patterns which evolved are illustrated in the top part of this figure. They are labeled a, b, c, d, and correspond to the similarly labeled data points in the bottom figure for $j^{\text{conv}}(t)$.

Some general features of the convective onset due to stochastic effects can also be described[9] by Eq. (1), with h now a noise source, which for simplicitly we will take as white, i.e.,

$$\langle h(t)\, h(t+\tau)\rangle = 2F\tau_0\delta(\tau) \tag{2}$$

The solution to Eq. (1) with this choice for h is shown as the dashed line in Fig. 5, and was able to reproduce the convective heat transport extremely well, with only F as an adjustable paramater. However, a deterministic field (i.e., a constant h) also yielded a reasonable fit to the heat transport data, as shown by the solid line in Fig. 5. Thus, the prime evidence for stochastic effects in the convective onset comes from the nature and the irreproducibility of the patterns.

The strength F of the stochastic force necessary to fit the experiment turns out to be larger than thermal noise in a Boussinesq system by four orders of magnitude.[9,17] One might thus conclude that the noise is of experimental origin and associated with the particular apparatus; however, deliberate large changes in the most obvious experimental noise source had no effect upon the results. Thus, at this time we regard the origin of the noise in the experiment as an unresolved issue.

Another experiment[14] which yielded evidence for stochastic effects in convective onset involved a time-periodic modulation of $\varepsilon(t)$ in the form

$$\varepsilon = \varepsilon_0 + \delta \cos \omega t$$

In this case a pattern would grow in strength and then fade away to the point of being unobservable during each cycle. It was found that an initial pattern was reproducible from one cycle to the next only if $\varepsilon_0 > \varepsilon_d(\delta, \omega)$. For smaller ε_0, random cellular flow such as that shown in Figs. 4 and 5 evolved after a few cycles and was irreproducible from one cycle to the next. Thus, in the ε_0 versus δ plane there is a deterministic region $\varepsilon_0 > \varepsilon_d$ and a stochastic region $\varepsilon_0 < \varepsilon_d$. The dividing line between the two in practice is quite sharp. Experimental results for $\varepsilon_d(\delta, 1)$ are shown in Fig. 6. These observations can in part also be described by Eq. (1). In the presence of modulation and for $\varepsilon_0 > 0$, the fixed-point solutions $A = \pm\varepsilon^{1/2}$ of the unmodulated system become limit cycles, and the unstable solution $A = 0$ is

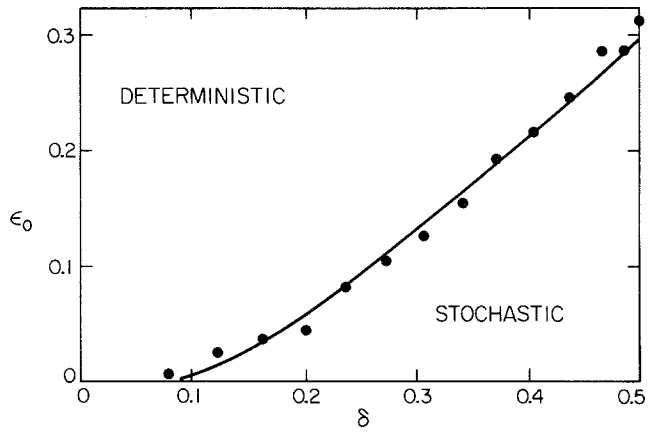

Fig. 6. The boundary between the deterministic and stochastic regions in the ε_0 versus δ plane of a Rayleigh–Bénard system under periodic modulation in the form $R/R_c = 1 + \varepsilon_0 + \delta \cos(\omega t)$. For this case, $\omega = 1$. Solid points: experimental results from ref. 14. Solid line: estimate from ref. 18 based on the Langevin equation, Eqs. (1) and (2), with a noise strength F taken from independent ramping experiments.[14]

the separatrix between the attractor basins of these limit cycles. In the presence of noise, the system can make transitions from one limit cycle to the other at random intervals. These transitions become more frequent as ε_0 decreases or δ increases because the limit cycles of the corresponding deterministic system approach the separatrix more closely. Swift and Hohenberg[18] have shown recently that the experimental data[14] for ε_d are

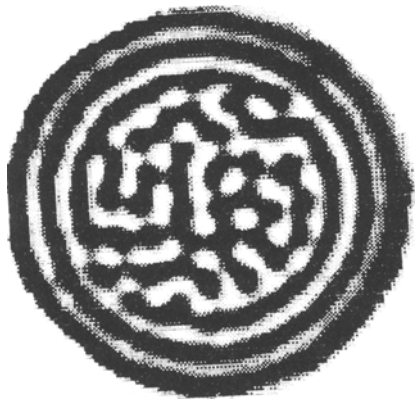

Fig. 7. An example of pattern competition between concentric rolls near dynamically forcing sidewalss and random cellular flow in the cell interior. This pattern was created by time-periodic modulation, with $\omega = 2$ and $\delta = 2.2$, and $\varepsilon_0 = 0.06$.

quantitatively consistent with Eq. (1) and a stochastic noise strength F equal to that determined from the ramping experiment[14] illustrated in Fig. 5. Their calculation of ε_d is shown as the solid line in Fig. 6. The agreement with the data clearly is quite good. This consistency between the two experiments within the framework of Eq. (1) lends further strength to the interpretation of the convective onset as a stochastic effect.

Finally, we want to emphasize the limitations of Eq. (1) as a model for the convective onset. This equation cannot of course explain the spatio-temporal complexity which is evident in Figs. 4 and 5. An example even more clearly beyond the scope of Eq. (1) is shown in Fig. 7. This figure corresponds to a modulation experiment with dynamically forcing sidewalls. For the parameters of this run, the deterministic forcing field penetrates only partly into the interior of the cell, and produces concentric rolls near the walls. In the cell interior the deterministic field is sufficiently weak to permit the stochastic field to dominate, thus yielding random cellular flow. It would be interesting to simulate this pattern competition, as well as the effects illustrated in Fig. 5, with model equations which contain appropriate gradient terms, such as the Swift–Hohenberg equation.[16]

ACKNOWLEDGMENTS

This work was supported by the Department of Energy under grant number DOE 87ER 13738.

REFERENCES

1. S. Chandrasekhar, *Hydrodynamic and Hydromagnetic Stability* (Oxford University Press, 1961).
2. R. E. Kelly and D. Pal, *J. Fluid Mech.* **86**:433 (1978); P. G. Daniels, *Proc. R. Soc. A* **358**:173 (1977); P. Hall and I. C. Walton, *Proc. R. Soc. A* **358**:199 (1977); E. L. Reiss, in *Application of Bifurcation Theory* (Academic Press, 1977), p. 37; S. N. Brown and K. Stewartson, *Proc. R. Soc. Lond. A* **360**:455 (1978); J. Tavantzis, E. L. Reiss, and B. Matkowsky, *SIAM J. Appl. Math.* **34**:322 (1978).
3. E. L. Koschmieder and S. G. Pallas, *Int. J. Heat Mass Transfer* **17**:991 (1974).
4. V. Steinberg, G. Ahlers, and D. S. Cannell, *Phys. Scripta* **32**:534 (1985); **T9**:97 (1985).
5. G. Ahlers, D. S. Cannell, and C. Meyer, unpublished; G. Ahlers, D. S. Cannell, and V. Steinberg, *Phys. Rev. Lett.* **54**:1373 (1985).
6. G. Ahlers, in *Fluctuations, Instabilities, and Phase Transitions*, T. Riste, ed. (Plenum, New York, 1975); *J. Fluid Mech.* **98**:137 (1980).
7. A. Aitta, G. Ahlers, and D. D. Cannell, *Phys. Rev. Lett.* **54**:673 (1985).
8. R. P. Behringer and G. Ahlers, *J. Fluid Mech.* **125**:219 (1982).
9. G. Ahlers, M. C. Cross, P. C. Hohenberg, and S. Safran, *J. Fluid Mech.* **110**:297 (1981).
10. G. Ahlers, P. C. Hohenberg, and M. Lücke, *Phys. Rev. Lett.* **53**:48 (1984); *Phys. Rev. A* **32**:3493, 4519 (1985).

11. M. C. Cross, P. C. Hohenberg, and M. C. Lücke, *J. Fluid Mech.* **136**:269 (1983).
12. M. S. Heutmaker, P. N. Fraenkel, and J. P. Gollub, *Phys. Rev. Lett.* **54**:1369 (1985); and references therein.
13. M. C. Cross, *Phys. Rev. A* **25**:1065 (1982); and references therein.
14. C. W. Meyer, G. Ahlers, and D. S. Cannell, *Phys. Rev. Lett.* **59**:1577 (1987).
15. V. M. Zaitsev and M. I. Shliomis, *Zh. Eksp. Teor. Fiz.* **59**:1583 (1970) [*Sov. Phys. JETP* **32**:866 (1971)]; R. Graham, *Phys. Rev. A* **10**:1762 (1974).
16. J. B. Swift and P. C. Hohenberg, *Phys. Rev. A* **15**:319 (1977).
17. H. van Beijeren and E. G. D. Cohen, *Phys. Rev. Lett.* **60**:1208 (1988).
18. J. B. Swift and P. C. Hohenberg, *Phys. Rev. Lett.* **60**:75 (1988).